

2-2-2008

Depinning and Plasticity of Driven Disordered Lattices

M. Cristina Marchetti
Syracuse University

Follow this and additional works at: <http://surface.syr.edu/phy>



Part of the [Physics Commons](#)

Repository Citation

arXiv:cond-mat/0503660v1

This Article is brought to you for free and open access by the College of Arts and Sciences at SURFACE. It has been accepted for inclusion in Physics by an authorized administrator of SURFACE. For more information, please contact surface@syr.edu.

Depinning and plasticity of driven disordered lattices

M. Cristina Marchetti

Physics Department, Syracuse University, Syracuse, NY 13244, USA

(Dated: February 2, 2008)

Invited lecture presented at the XIX Sitges Conference on *Jamming, Yielding, and Irreversible Deformations in Condensed Matter*, Sitges, Barcelona, Spain, June 14-18, 2004.

I. INTRODUCTION

Nonequilibrium transitions from stuck to flowing phases underlie the physics of a wide range of physical phenomena. In a first class of systems the onset of a stuck or frozen state occurs as a result of intrinsic dynamical constraints, due to interactions or crowding, and is usually referred to as *jamming* [1]. Familiar examples are supercooled liquids that become a glasses upon lowering the temperature, colloidal suspensions that undergo a glass transition due to crowding upon increasing the density or the pressure, foams and granular materials that jam under shear, arrays of dislocations in solids that jam under an applied load. In a second class of systems the transition to a stuck state is due to external constraints, such as the coupling to quenched disorder (pinning centers from material defects in vortex lattices, optical traps in colloids, etc.), and is denoted as *pinning* [2]. Both classes of systems can be driven in and out of glassy states by tuning not only temperature, density or disorder strength, but also an applied external force. The external drive may be a shear stress in conventional glasses or simply a uniform applied force in systems with extrinsic quenched disorder, where even a uniform translation of the system relative to the fixed impurities represents a nontrivial perturbation. Vortex lattices in superconductors [3] and charge density waves (CDWs) in metals [4] can be driven in and out of stuck glassy states by a uniform external current or electric field, respectively. As recognized recently in the context of jamming, the external drive plays a role not unlike that of temperature in driving the system to explore metastable configurations and should be included as an axis in a complete phase diagram.

In this lectures I will focus on zero-temperature depinning transitions of interacting condensed matter systems that spontaneously order in periodic structures and are driven over quenched disorder. The prototype examples are vortex lattices in type-II superconductors [5] and charge density waves in anisotropic metals [8]. Other examples include Wigner crystals of two dimensional electrons in a magnetic field moving under an applied voltage [6], lattices of magnetic bubbles

moving under an applied magnetic field gradient [7], and many others. In general these systems form a lattice inside a solid matrix, provided by the superconducting or conducting material and are subject to pinning by random impurities. The statics of such disordered lattices have been studied extensively [5]. One crucial feature that distinguishes the problem from that of disordered interfaces is that the pinning force experienced by the periodic structure is itself periodic, although with random amplitude and phase [9]. As a result, although disorder always destroys true long-range translational order and yields glassy phases with many metastable states and diverging energy barriers between these states, the precise nature of the glassy state depends crucially on disorder strength. At weak disorder the system, although glassy, retains topological order (the resulting phase has been named Bragg glass in the context of vortex lattices) [9]. Topological defects proliferate only above some characteristic disorder strength, where a topologically disordered glass is formed.

The driven dynamics of disordered periodic structures have been studied extensively by modeling the system as an overdamped elastic medium that can be deformed by disorder, but is not allowed to tear, that is by neglecting the possible formation of topological defects due to the competition of elasticity, disorder and drive. This model, first studied in the context of charge density waves, exhibits a nonequilibrium phase transition from a pinned to a *unique* sliding state at a critical value F_T of the driving force. This nonequilibrium transition displays universal critical behavior as in equilibrium *continuous* transitions, with the medium's mean velocity v acting as an order parameter [2, 8, 10]. While the overdamped elastic medium model may seem adequate to describe the dynamics of driven Bragg glasses, many experiments and simulations of driven systems have shown clearly that topological defects proliferate in the driven medium even for moderate disorder strengths [11, 12, 13, 14, 54]. The dynamics near depinning becomes spatially and temporally inhomogeneous, with coexisting moving and pinned degrees of freedom. This regime has been referred to as plastic flow and may be associated with memory effects and even hysteresis in the macroscopic response.

The goal of the present lectures is to describe coarse-grained models of driven extended systems that can lead to history-dependent dynamics. Such models can be grouped in two classes. In the first class the displacement of the driven medium from some undeformed reference configuration remains single-valued, as appropriate for systems without topological defects, but the interactions are modified to incorporate non-elastic restoring forces [15, 16, 17, 18, 19, 20]. In the second class of models topological defects are explicitly allowed by removing the constraint of single-valued displacements [21, 22, 23]. Here we will focus on the first class and specifically consider driven

periodic media with a linear stress-strain relation, where the stress transfer between displacements of different parts of the medium is nonmonotonic in time and describes viscous-type slip of neighboring degrees of freedom. A general model of this type that encompasses many of the models discussed in the literature was proposed recently by us [18, 20, 24]. Here slips between neighboring degrees of freedom are described as viscous force, that allows a moving portion of the medium to overshoot a static configuration before relaxing back to it. It is shown below that such viscous coupling can be considered an effective way of incorporating the presence of topological defects in the driven medium. Related models have also been used to incorporate the effect of inertia or elastic stress overshoot in crack propagation in solids [19, 25]. The precise connection between the two classes of models has been discussed in Ref. [26].

In Section II we review the simplest example of depinning transition, obtained when non-interacting particles are driven through a periodic pinning potential. By contrasting the case of periodic and non-periodic pinning, we stress that care must be used in the definition of the mean velocity of the system. In Section III, we first describe the generic coarse-grained model of a driven elastic medium that exhibits a *continuous* depinning transition as a function of the driving force from a static to a *unique* sliding state. Next we introduce an anisotropic visco-elastic model as a generic model of a periodic system driven through strong disorder. The model considers coarse-grained degrees of freedom that can slip relative to each other in the directions transverse to the mean motion, due to the presence of small scale defects (phase slips, dislocations, grain boundaries) at their boundaries, but remain elastically coupled in the longitudinal directions. The slip interactions are modeled as viscous couplings and a detailed physical motivation for this choice is given in section III C. Most of our current results for these type of models are for the mean-field limit and are presented in Section IV. The studies carried out so far for finite-range interactions suggest that the mean-field theory described here may give the correct topology for the phase diagram, although there will of course be corrections to the critical behavior in finite dimensions [27]. Finally, we conclude in Section V by discussing the relation to other models described in the literature and the connection to experiments.

II. DEPINNING OF NONINTERACTING PARTICLES

It is instructive to begin with the problem of a single particle driven through a *periodic* pinning potential as the simplest illustration of driven depinning. Assuming overdamped dynamics, the

equation of motion for the position x of the particle is

$$\zeta \frac{dx}{dt} = F + hY(x), \quad (1)$$

where ζ is a friction coefficient (in the following we choose our units of time so that $\zeta = 1$), F is the external drive and $Y(x) = Y(x + n)$, with n an integer, is a periodic function of period 1. For simplicity we choose a piecewise linear pinning force, corresponding to $Y(x) = (1/2 - x)$, for $0 \leq x \leq 1$. In this case a periodic solution of Eq. (1) is obtained immediately in terms of the time T needed to traverse a potential well, or period. Introducing an arbitrary time t_J such that if $x(t_J) = n$, then $x(t_J + T) = n + 1$, the particle position for $t_J + nT \leq t \leq t_J + (n + 1)T$ is

$$x(t) = n + \frac{1 - e^{-h(t-t_J-nT)}}{1 - e^{-hT}}, \quad (2)$$

where T is given by

$$T(h) = \frac{1}{h} \ln \left(\frac{2F + h}{2F - h} \right), \quad (3)$$

for $F > h/2$ and diverges for $F < h/2$. In other words if $F < h/2$ the particle never leaves the initial well, i.e., it is pinned. The threshold force for depinning is then $F_c = h/2$. In the sliding state the mean velocity is defined as the average of the instantaneous velocity $v(t) = \frac{dx}{dt}$ over the arbitrary initial time t_J . This gives

$$\bar{v} \equiv \langle v \rangle_{t_J} = \int_{t-(n+1)T}^{t-nT} \frac{dt_J}{T} v(t) = \frac{1}{T}. \quad (4)$$

This definition naturally identifies the mean velocity of the particle with the inverse of the period. The logarithmic behavior of \bar{v} near threshold, $\bar{v} \sim -1/\ln(F_c - F)$, is peculiar to a discontinuous pinning force. For an arbitrary pinning force $Y(X)$ the period T is

$$T = \int_0^1 dx \frac{1}{F + hY(x)}, \quad (5)$$

and can be evaluated analytically for various forces. For instance, for a sinusoidal pinning force, $Y(x) = \sin(2\pi x)$, one finds $T = (F^2 - h^2)^{-1/2}$, which gives $\bar{v} \sim (F - F_c)^{1/2}$ near threshold, a generic behavior for continuous pinning forces.

The main focus of the remainder of this paper will be on the modeling of extended driven systems as collections of interacting degrees of freedom. It will then be important to distinguish two cases. For extended systems that are periodic, such as charge density waves and vortex lattices, the pinning potential is itself periodic as each degrees of freedom sees the same disorder after advancing one lattice constant. For non-periodic systems, such as interfaces, each degree of

freedom moves through a random array of defects. When interactions are neglected, an extended *periodic* system moving through a periodic random pinning potential can be modeled as a collection of N non-interacting particles, where each particle sees its own periodic pinning potential. The pinning potentials seen by different particles may differ in height and be randomly shifted relative to each other, as sketched in Fig. 1. The equation of motion for the i -th particle at position x_i is then

$$\frac{dx_i}{dt} = F + h_i Y(x_i + \gamma_i), \quad (6)$$

where γ_i are random phases uniformly distributed in $[0, 1)$ and the pinning strengths h_i are drawn independently from a distribution $\rho(h_i)$. Since the displacements x_i are decoupled, they can be indexed by their disorder parameters γ and h instead of their spatial label i , i.e., $x_i(t; \gamma_i, h_i) \rightarrow x(t; \gamma, h)$. The mean velocity of the many-particle system can then be written as an average over the random phases and pinning strengths,

$$\begin{aligned} \bar{v} &= \frac{1}{N} \sum_i v_i = \langle v(t; \gamma, h) \rangle_{\gamma, h} \\ &= \int dh \rho(h) \int_0^1 d\gamma v(t; \gamma, h), \end{aligned} \quad (7)$$

where $v(t; \gamma, h) = \frac{dx(t; \gamma, h)}{dt}$. The average over the random phase of each degree of freedom is equivalent to the average over the random time shift t_J described for the single-particle case and yields $\int_0^1 d\gamma v(t; \gamma, h) = 1/T(h)$, with $T(h)$ the period of each particle given in Eq. (3). The mean velocity is then

$$\bar{v} = \left\langle \frac{1}{T(h)} \right\rangle_h, \quad (8)$$

where $\langle \dots \rangle_h = \int dh \dots \rho(h)$ denotes the average over the barrier height distribution. For distributions $\rho(h)$ that have support at $h = 0$, a system of *noninteracting* particles with periodic pinning depins at $F = 0$, as there are always some particles experiencing zero pinning force.

A different single-particle problem that has been discussed in the literature is that of a particle moving through a *random (non-periodic)* array of defects [28]. The defects can be described as pinning potential wells centered at random positions and/or with random well heights. To make contact with the periodic case we consider a particle moving through a succession of evenly spaced pinning potential wells of random heights. The equation of motion is

$$\partial_t x = F + \sum_{p=0}^{N_p-1} h_p Y(x - p), \quad (9)$$

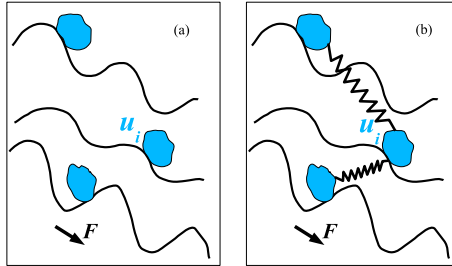


FIG. 1: (a) Sketch of noninteracting degrees of freedom driven over a random periodic pinning potential in one dimension. Spatial coordinates have been discretized so that degrees of freedom are labelled by an index i . In (b) the case where each degree of freedom interacts elastically with its neighbors is shown. This is a discretized one-dimensional realization of the elastic medium model described by Eq. (13) below.

where N_p is the total number of pinning centers and the pinning strengths h_p are drawn independently from a distribution $\rho(h_p)$. Choosing again the piecewise-linear pinning force, the time to traverse the p -th well is simply $T(h_p)$, with T given by Eq. (3). The mean velocity of the particle is defined as the total distance travelled divided by the total time and is given by

$$\bar{v} = \frac{N_p}{\sum_p T(h_p)} \equiv \frac{1}{\langle T(h) \rangle_h}. \quad (10)$$

In this case, unless the distribution $\rho(h)$ is bounded from above, there is always a finite probability that the particle will encounter a sufficiently deep potential well to get pinned. Therefore for unbounded $\rho(h)$ the particle is always pinned in the thermodynamic limit. If $\rho(h)$ is bounded from above by a maximum pinning strength h_{\max} , this value also represents the depinning threshold. Finally, the case of many noninteracting particles driven through a random array of defects is equivalent to that of a single particle, as the mean velocity of each particle can be calculated independently. The mean velocity of the system is then again given by Eq. (10).

III. DEPINNING OF AN EXTENDED MEDIUM

We consider a d -dimensional periodic structure driven along one of its symmetry directions, chosen as the x direction. The continuum equations for such a driven lattice within the elastic approximation were derived by various authors by a rigorous coarse-graining procedure of the microscopic dynamics [29, 30, 31]. Assuming overdamped microscopic dynamics, the equation for the local deformation $\mathbf{u}(\mathbf{r}, t)$ of the medium (in the laboratory frame) from an undeformed reference state is written by balancing all the forces acting on each portion of the system as [32]

$$\partial_t u_i = \partial_j \sigma_{ij} + F \delta_{ix} + F_{pi}(\mathbf{r}, \mathbf{u}), \quad (11)$$

where σ_{ij} is the stress tensor due to interactions among neighboring degrees of freedom, F is the driving force and \mathbf{F}_p is the periodic pinning force. The periodicity of the pinning force, which contains Fourier components at all the reciprocal lattice vectors of the lattice, arises from the coupling to the density of the driven lattice.

A. Elastic model

For conventional short-ranged elasticity the stress tensor is

$$\sigma_{ij}^{\text{el}} = 2c_{66}u_{ij} + \delta_{ij}(c_{11} - c_{66})u_{kk} , \quad (12)$$

where c_{11} and c_{66} are the compressional and shear moduli of the driven lattice, respectively, and $u_{ij} = \frac{1}{2}(\partial_i u_j + \partial_j u_i)$ is the strain tensor. It was shown in Ref. [29] that deformations of the driven lattice along the direction of the driving force grow without bound due to large transverse shear stresses that generate unbounded strains responsible for dislocation unbinding. For this reason, we focus here on the dynamics of a scalar field $u_x(x, \mathbf{y}, t) \equiv u(\mathbf{r}, t)$, with $\mathbf{r} = (x, \mathbf{y})$, describing deformations of the driven lattice along the direction of mean motion. The $d-1$ -dimensional vector \mathbf{y} denotes the coordinates transverse to the direction of motion. Assuming $c_{11} \gg c_{66}$, we obtain a scalar model for the driven elastic medium, given by

$$\partial_t u = c_{11} \partial_x^2 u + c_{66} \nabla_{\mathbf{y}}^2 u + F + F_p(\mathbf{r}, u) , \quad (13)$$

where F_p denotes the x component of the pinning force. For simplicity we also consider a model that only retains the component of the pinning force at the smallest reciprocal lattice vector and choose our units of lengths so that the corresponding period is 1. The pinning force is then taken of the form

$$F_p(\mathbf{r}, u) = h(\mathbf{r})Y(u(\mathbf{r}, t) - \gamma(\mathbf{r})) , \quad (14)$$

where $Y(u) = Y(u + n)$ is a periodic function. The random pinning strengths h are drawn independently at every spatial point from a distribution with zero mean and short-ranged correlations to be prescribed below. The random phases γ are spatially uncorrelated and distributed uniformly in $[0, 1)$.

The model of a driven overdamped elastic medium embodied by Eq. (13) has been studied extensively both analytically and numerically [2, 8, 10, 33, 34]. It exhibits a depinning transition at a critical value F_T of the applied force from a static to a *unique* sliding state [35]. The depinning

can be described as a continuous equilibrium transition, with the mean velocity $\bar{v} = \langle \partial_t u \rangle$ playing the role of the order parameter, and universal critical behavior. The velocity vanishes as F_T is approached from above as $\bar{v} \sim (F - F_T)^\beta$. The critical exponent β depends only on the system dimensionality and was found to be $\beta = 1 - \epsilon/6 + \mathcal{O}(\epsilon^2)$ using a functional RG expansion in $\epsilon = 4 - d$ [10, 36].

B. Viscoelastic model

Strong disorder can yield topological defects in the driven lattice, making the elastic model inapplicable [37, 38]. In this case the dynamics becomes inhomogeneous, with coexisting pinned and moving regions [39, 40]. The depinning transition may be discontinuous (first order), possibly with macroscopic hysteresis. Several mean-field models of driven extended systems have been proposed [2, 16, 17, 18, 19, 21, 22] to describe this inhomogeneous dynamics. Here we focus on a class of models that retains a single-valued displacement field and a linear stress-strain relation, but assumes that the presence of topological defects can be effectively incorporated at large scales by a non-instantaneous stress transfer that couples to gradients of the local velocity (rather than displacement). More precisely, we consider an anisotropic model of coarse-grained degrees of freedom that can slip relative to each other in at least one of the directions transverse to the mean motion, due to the presence of small scale defects (phase slips, dislocations, grain boundaries) at their boundaries, but remain elastically coupled in the longitudinal directions [20]. This model incorporates the anisotropy of the sliding state in the plastic flow region that results either from flow along coupled channels oriented in the direction of the drive (e.g., as in the moving smectic phase [41]) or in layered materials such as the high- T_c cuprate superconductors. It also encompasses several of the models discussed in the literature.

For generality, consider a $d = d_{\parallel} + d_{\perp}$ -dimensional medium composed of degrees of freedom that are coupled elastically in d_{\parallel} direction and can slip relative to each other in the remaining d_{\perp} directions. The axis x along which the driving force is applied is along one of the d_{\parallel} directions. The equation of motion for the displacement $u(\mathbf{r}_{\parallel}, \mathbf{r}_{\perp}, t)$ is given by

$$\partial_t u = K \nabla_{\parallel}^2 u + \eta \nabla_{\perp}^2 v + F + F_p(\mathbf{r}, u);, \quad (15)$$

with $v = \partial_t u$ the local velocity. This model will be referred to as the visco-elastic (VE) model as it incorporates elastic couplings of strength K in d_{\parallel} directions and viscous couplings of strength controlled by a shear viscosity η in the remaining d_{\perp} directions. A two-dimensional cartoon of this

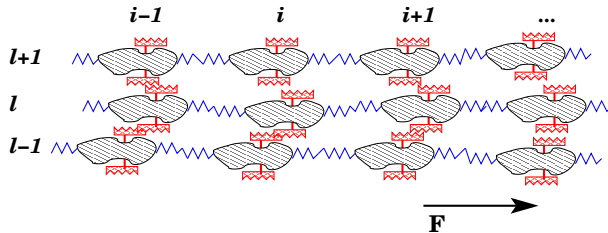


FIG. 2: A two-dimensional realization of the anisotropic driven medium described in the text. Spatial coordinates have been discretized in the figure so that degrees of freedom are labelled by indices ℓ and i , respectively transverse and longitudinal to the direction of the driving force, F . Each degree of freedom interacts with its neighbors via elastic couplings in the longitudinal direction and via viscous or similar slip couplings in the transverse direction.

anisotropic model is shown in Fig. 2.

For $\eta = 0$ (or $d_{\perp} = 0$) the VE model reduces to the elastic model (but with isotropic elasticity) of Eq. (13). Conversely, for $K = 0$ (or $d_{\parallel} = 0$) Eq. (15) reduces to the purely viscous model studied earlier by us [18, 24]. For any distribution of pinning strengths with support at $h = 0$, the purely viscous model has zero threshold for depinning, but it does exhibit a critical point separating regions of unique and multivalued solutions for the mean velocity. In the VE model ($\eta \neq 0$ and $K \neq 0$) even when fluid-like shear takes place, particle conservation gives a sharp depinning transition in flow along the channels. Furthermore, as shown below, the model has a sharp mean-field tricritical point separating a region of parameters where depinning is continuous, in the universality class of elastic depinning, from one where depinning become discontinuous and hysteretic.

It is important to stress that the VE model still assumes *overdamped microscopic dynamics*. Velocity or viscous couplings can appear generically in the large-scale equations of motion upon coarse-graining the microscopic dynamics of a dissipative medium. In fact, next we show that viscous couplings indeed represent an effective way of incorporating the local dissipation due to the presence of topological defects.

C. Viscoelastic coupling as an effective description of topological defects

The goal of this section is to provide some justification to the anisotropic VE model as an effective description of topological defects in a driven lattice. To this purpose we consider a two dimensional medium and take advantage of the continuum equations developed many years ago by Zippelius et al. [42] to describe the time-dependent properties of two-dimensional solids near

melting. These authors combined the equations of free dislocation motion with solid hydrodynamics to construct a semimicroscopic dynamical model of a solid with free dislocations. They further showed that the dynamics of such of a "heavily dislocated solid" (an elastic medium with an equilibrium concentration of free dislocations) is identical to that of the hexatic phase obtained when a two-dimensional solid melts via the unbinding of dislocations [43]. More recently we [44] reconsidered the dynamical equations for the "heavily dislocated solid" of Ref. [42] and showed that they can be recast in the form of the phenomenological equations of a viscoelastic fluid (with hexatic order) introduced many years ago by Maxwell [45]. In the presence of free dislocations the local stresses in the medium have contributions from both elastic stresses and defect motion. The latter couple again to the the local strains which control the defect dynamics. By eliminating the defect degrees of freedom, one obtains a linear, although nonlocal, relation between strain and stress, given by [46]

$$\begin{aligned} \sigma_{ij}^{\text{VE}}(\mathbf{r}, t) = & \delta_{ij} c_L u_{kk}(\mathbf{r}, t) + \delta_{ij}(c_{11} - c_L) \int_{-\infty}^t dt' e^{-(t-t')/\tau_b} v_{kk}(\mathbf{r}, t') \\ & + 2c_{66} \int_{-\infty}^t dt' e^{-(t-t')/\tau_s} [v_{ij}(\mathbf{r}, t') - \frac{1}{2}\delta_{ij}v_{kk}(\mathbf{r}, t')] , \end{aligned} \quad (16)$$

where $v_{ij} = \frac{1}{2}(\partial_i v_j + \partial_j v_i)$ and the velocity \mathbf{v} is defined here in terms of the momentum density \mathbf{g} as $\mathbf{v} = \mathbf{g}/\rho_0$, with ρ_0 the equilibrium mass density of the medium. Also in Eq. (16) c_L is the compressional modulus of the liquid and $\tau_b \approx (c_{11}\mu_d^c n_f a_0^2)^{-1}$ and $\tau_s \approx (c_{66}\mu_d^g n_f a_0^2)^{-1}$ are the compressional and shear relaxation times, with $\mu_d^{g,c}$ the dislocation glide and climb mobility, respectively. Of course in the presence of dislocations the displacement u is no longer single-valued (although the strain u_{ij} remains single-valued and continuous) and $\partial_t u \neq v$ due to both the motion of vacancy/interstitial defects and of dislocations. The phenomenological Maxwell model of viscoelasticity is obtained by assuming that $\partial_t u = v$ even in the presence of dislocations. Then for $t \ll \tau_s, \tau_b$ the viscoelastic stress $\sigma^{\text{VE}}(\mathbf{r}, t)$ reduces to the familiar elastic stress tensor given in Eq. (12),

$$\sigma^{\text{VE}}(\mathbf{r}, t \ll \tau_s, \tau_b) \approx \sigma_{ij}^{\text{el}} . \quad (17)$$

Conversely for $t \gg \tau_s, \tau_b$ one obtains

$$\sigma_{ij}^{\text{VE}}(\mathbf{r}, t \gg \tau_s, \tau_b) \approx \delta_{ij} c_L u_{kk} + \delta_{ij}(\eta_b + \eta)v_{kk} + 2\eta v_{ij} , \quad (18)$$

which describes stresses in a viscous fluid of shear viscosity $\eta = c_{66}\tau_s$ and bulk viscosity $\eta_b = (c_{11} - c_L)\tau_b$. The first term on the right hand side of Eq. (18) is the pressure and incorporates the fact that even a liquid has a nonzero long-wavelength compressional elasticity, which is associated

with density conservation. As we will see below this terms plays a crucial role in controlling the physics of depinning of a viscoelastic medium. The Maxwell viscoelastic fluid has solid-like shear rigidity at high frequency, but flows like a fluid at low frequency. Since the relaxation times τ_s and τ_b are inversely proportional to the density n_f of free dislocations, the Maxwell model behaves as a continuum elastic medium on all time scales when $n_f \rightarrow 0$ and as a viscous fluid when $n_f a_0^2 \sim 1$.

Dislocation climb is much slower than dislocation glide ($\mu_d^c \ll \mu_d^g$), resulting in $\tau_b \gg \tau_s$. We therefore assume that the response to compressional deformations is instantaneous on all time scales, but retain a viscoelastic response to shear deformations. Letting $\tau_b \rightarrow \infty$, we find

$$\sigma_{ij}^{\text{VE}}(\mathbf{r}, t) \approx \delta_{ij} c_{11} u_{kk}(t) + 2c_{66} \int_{-\infty}^t dt' e^{-(t-t')/\tau_s} [v_{ij}(t') - \frac{\delta_{ij}}{2} v_{kk}(t')]. \quad (19)$$

We now turn to the case of interest here, where topological defects are generated in a an extended medium driven through quenched disorder. In this case the medium has no low frequency shear modulus, but particle conservation still requires long wavelength elastic restoring forces to *compressional* deformations. On the other hand, the number of topological defects is not fixed as dislocations are continuously generated and annihilated by the interplay of elasticity, disorder and drive [39, 40, 47]. Furthermore, unbound dislocations can be pinned by disorder and do not equilibrate with the lattice. In the plastic region near depinning the dynamics remains very inhomogeneous and fluid-like and the pinning of dislocations by quenched disorder is not sufficient to restore the long wavelength shear-stiffness of the medium. For this reason we propose to describe the effect of topological defects near depinning by replacing elastic *shear* stresses by viscoelastic ones, while retaining elastic *compressional* forces. Of course the resulting model that assumes a fixed density of dislocations becomes inapplicable at large driving forces where dislocations heal as the lattice reorders. For the case of interest here of a scalar model describing only deformations along the direction of motion, the viscoelastic model of a driven disordered medium is

$$\partial_t u = c_{11} \partial_x^2 u + c_{66} \int_{-\infty}^t dt' e^{-(t-t')/\tau_s} \partial_y^2 v(t') + F + h(\mathbf{r})Y(u - \gamma(\mathbf{r})), \quad (20)$$

with $v = \partial_t u$. This model naturally incorporates the anisotropy and channel-like structure of the driven medium, where *shear* deformations due to gradients in the displacement in the directions transverse to the mean motion ($\partial_y u \neq 0$) are most effective at generating the large stresses responsible for the unbinding of topological defects. It is instructive to note that due to the exponential form of stress relaxation the integro-differential equation (20) is equivalent to a second order differential equation for the displacement,

$$\tau_s \partial_t^2 u + \gamma_{\text{eff}} \partial_t u = c_{11} \partial_x^2 u + \eta \partial_y^2 v + F + h(\mathbf{r})Y(u - \gamma(\mathbf{r})), \quad (21)$$

with γ_{eff} an effective friction [18]. In other words the effect of a finite density of dislocations in the driven lattice yields "inertial effects" on a scale controlled by the time $\tau_s \sim 1/n_f$. The purely viscous model obtained from Eq. (21) with $c_{11} = 0$ was analyzed in detail in Ref. [24] where it was shown that if τ_s and $\eta = c_{66}\tau_s$ are tuned independently, then τ_s is a strongly irrelevant parameter in the RG sense. This allows us to consider a simplified form of the equation for the driven medium obtained from Eq. (21) with $\tau_s = 0$, but $\eta = c_{66}\tau_s$ finite, leading to the general anisotropic viscoelastic model introduced in Eq. (15).

IV. MEAN-FIELD SOLUTION

The mean-field approximation for the VE model is obtained in the limit of infinite-range elastic and viscous interactions. To set up the mean field theory, it is convenient to discretize space in both the transverse and longitudinal directions, using integer vectors i for the d_{\parallel} -dimensional intra-layer index and ℓ for the d_{\perp} -dimensional layer index. The local displacement along the direction of motion is $u_{\ell}^i(t)$. Its dynamics is governed by the equation,

$$\partial_t u_{\ell}^i = \sum_{\langle j \rangle} K_{ij} (u_{\ell}^i - u_{\ell}^j) + \sum_{\langle m \rangle} \eta_{\ell m} [\dot{u}_{\ell}^i - \dot{u}_{\ell}^m] + F + h_{\ell}^i Y(u_{\ell}^i - \gamma_{\ell}^i), \quad (22)$$

where the dot denotes a time derivative and $\langle j \rangle$ ($\langle m \rangle$) ranges over sites j (m) that are nearest neighbor to i (ℓ). The random pinning strengths h_{ℓ}^i are chosen independently with probability distribution $\rho(h_{\ell}^i)$ and the γ_{ℓ}^i are distributed uniformly and independently in $[0, 1)$. For a system with $N = N_{\parallel} \times N_{\perp}$ sites, *one* mean field theory is obtained by assuming that all sites are coupled with uniform strength, both within a given channel and with other channels. Each discrete displacement then couples to all others only through the mean velocity, $\bar{v} = N^{-1} \sum \dot{u}_{\ell}^i$, and the mean displacement, $\bar{u} = N^{-1} \sum u_{\ell}^i$. We assume that the disorder is isotropic and the system is self averaging and look for solutions moving with stationary velocity: $\bar{u} = \bar{v}t$. Since all displacements u are coupled, they can now be indexed by their disorder parameters γ and h , rather than the spatial indices i and ℓ . The mean-field dynamics is governed by the equation

$$(1 + \eta)\dot{u}(\gamma, h) = K(\bar{v}t - u) + F + \eta\bar{v} + hY(u - \gamma). \quad (23)$$

The cases $K = 0$ and $K \neq 0$ need to be discussed separately.

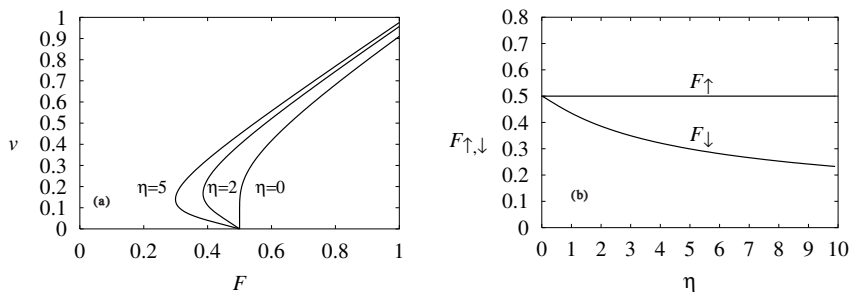


FIG. 3: (a) Velocity versus driving force for the purely viscous model ($K = 0$, $\eta \neq 0$) with a narrow distribution of pinning strength, $\rho(h) = \delta(h - 1)$, for $\eta = 0, 2, 5$. There is a finite depinning threshold at $F_T = 1/2$. In (b) the depinning and repinning forces F_{\uparrow} and F_{\downarrow} are shown as functions of η .

A. Mean-field theory for viscous model: $K = 0$, $\eta \neq 0$

When $K = 0$, the mean field equation becomes identical to that of a single particle discussed in Section II driven by an effective force $F + \eta\bar{v}$ (with friction $1 + \eta$). In this case different degrees of freedom move at different velocities even in the mean field limit. The mean field velocity is determined by the self-consistency condition $\bar{v} = \langle \dot{u} \rangle_{\gamma, h}$, where the average over the random phases is equivalent to the average over the random times shifts t_J given in Eq. (4). For the case of a piecewise linear pinning force using Eq. (8) we find

$$\bar{v} = \frac{1}{1 + \eta} \int dh \rho(h) \frac{1}{T(h, F + \eta\bar{v})}, \quad (24)$$

with $T(h, F)$ given by Eq. (3). The mean velocity obtained by self-consistent solution of Eq. (24) is shown in Figs. 3 and 4 for two distributions of pinning strengths.

For a narrow distribution, $\rho(h) = \delta(h - 1)$, there is a finite threshold $F_T = 1/2$, independent of η . The velocity is multivalued for any finite η . When the force is ramped up adiabatically from the static state the system depins at $F_{\uparrow} = F_T$. When the force is ramped down from the sliding state, the system repins at the lower value $F_{\downarrow}(\eta)$. The depinning and repinning forces are shown in Fig. 3(b). The region where unique and multivalued velocity solutions coexist extend to $\eta = 0$. For a broad distribution with support at $h = 0$, e.g., $\rho(h) = e^{-h}$, the threshold for depinning is zero as some of the degrees of freedom always experience zero pinning and start moving as soon as a force is applied. There is a critical point at (F_c, η_c) . For $\eta > \eta_c$ the analytical solution for $\bar{v}(F)$ is multivalued, as shown in Fig. 4. If the force is ramped up adiabatically from zero at a fixed $\eta > \eta_c$, the system depins discontinuously at $F_{\uparrow}(\eta)$, while when the force is ramped down it repins at the lower value $F_{\downarrow}(\eta)$, as shown in Fig. 4. The viscous model has also been studied in finite dimensions

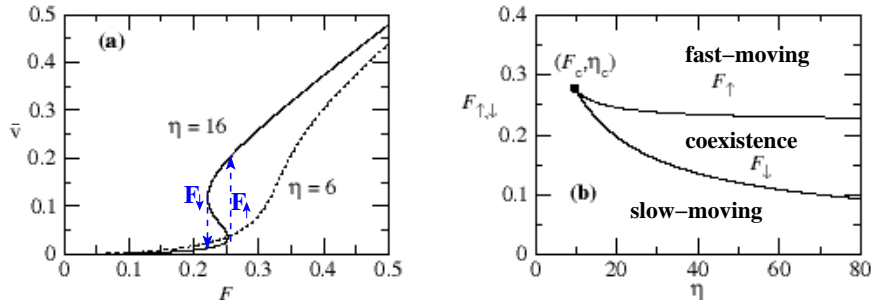


FIG. 4: (a) Velocity versus driving force for the purely viscous model ($K = 0$, $\eta \neq 0$) with a broad distribution of pinning strength, $\rho(h) = e^{-h}$ for $\eta = 6, 16$. In this case there are no stable static (pinned states). The velocity is single valued for $\eta < \eta_c$ and multi-valued for $\eta > \eta_c$. In this case when F is ramped up from zero, the velocity jumps discontinuously at F_\uparrow where the system goes from the "slow-moving" to the "fast-moving" state. Here and below "coexistence" refers to multistability of the solutions to the equations of motion. When F is then ramped down from within the fast-moving state the jump in \bar{v} occurs at the lower value F_\downarrow . The forces F_\downarrow and F_\uparrow become equal at the critical point, as shown in frame (b).

by mapping it onto the nonequilibrium random field Ising model (RFIM) [24]. In the mapping, the local velocities correspond to spin degrees of freedom, the driving force is the applied magnetic field and the mean velocity maps onto the magnetization. The RFIM has a critical point separating a region where the magnetization versus applied field curve displays hysteresis with a discontinuous jump to a region where there is no jump in the hysteresis curve [48, 49]. In the viscous model the critical point separates a region where the velocity curve is smooth and continuous from the region where the "depinning" (from "slow-moving" to "fast-moving" states) is discontinuous and hysteretic. The critical point is in the Ising universality class, with an upper critical dimension $d_c = 6$.

B. Mean-field theory for VE model: $K \neq 0$ and $\eta \neq 0$

When $K \neq 0$, all degrees of freedom are coupled by a spring-like interaction (the first term on the right hand side of Eq. (23)) to the mean field $\bar{u} = \bar{v}t$ and cannot lag much behind each other. This forces all the periods to be the same, independent of h , and yields a nonvanishing threshold for depinning. In this case the mean field velocity is determined by imposing $\langle u(t; \gamma, h) - \bar{v}t \rangle_{\gamma, h} = 0$.

It is useful to first review the case where $K \neq 0$ and $\eta = 0$. In this limit, Eq. (23) reduces to the mean field theory of a driven elastic medium worked out by Fisher and collaborators [10]. No moving solution exists above a finite threshold force F_T . For the piecewise linear pinning force this

is given by

$$F_T = \left\langle \frac{h^2}{2(K+h)} \right\rangle_h. \quad (25)$$

For $F > F_T$ there is a *unique* moving solution that has a universal dependence on F near F_T , where it vanishes as $\bar{v} \sim (F - F_T)^\beta$. In mean-field the critical exponent β depends on the shape of the pinning force: $\beta = 1$ for the discontinuous piecewise linear force and $\beta = 3/2$ for generic smooth forces. Using a functional RG expansion in $\epsilon = 4 - d$, Narayan and Fisher [10] showed that the discontinuous force captures a crucial intrinsic discontinuity of the large scale, low-frequency dynamics, giving the general result $\beta = 1 - \epsilon/6 + \mathcal{O}(\epsilon^2)$, in reasonable agreement with numerical simulations in two and three dimensions [33, 34]. For simplicity and to reflect the ‘‘jerkiness’’ of the motion in finite-dimensional systems at low velocities, we use piecewise linear pinning below.

When $\eta > 0$ the nature of the depinning differs qualitatively from the $\eta = 0$ case, in that hysteresis in the dynamics can take place. Again, no self-consistent moving solution exists for $F < F_T$, with F_T independent of η . Above threshold, both unique and multi-valued moving solutions exist, depending on the values of the parameters: η , K , and the shape of the disorder distribution, $\rho(h)$. To obtain the mean field solution in the sliding state, we examine the motion during one period $T = 1/\bar{v}$ during which the displacement advances by 1. Eq. (23) is easily solved for $0 \leq u \leq 1$ and $\gamma = 0$, with the result,

$$u(t; \gamma = 0, h) = \frac{K\bar{v}t + F + \eta\bar{v} + h/2}{(1 + \eta)\lambda} - \frac{K\bar{v}}{(1 + \eta)\lambda^2} + Ae^{-\lambda t}, \quad (26)$$

where $\lambda = (K + h)/(1 + \eta)$. At long times, regardless of the initial condition, $u(t)$ approaches a periodic function of period $T = 1/\bar{v}$ with jumps in its time derivative at times $t_J + nT$, with n an integer. The constant A is determined by requiring that if $u(t_J + nT) = n$, then $u(t_J + (n + 1)T) = n + 1$. Writing $u(t; \gamma, h) = \bar{v}t + \tilde{u}$, it is easy to see that for an arbitrary value of γ , the solution \tilde{u} will have the form $\tilde{u} = \tilde{u}(\bar{v}t - \gamma, h)$. The mean velocity is then obtained from $\langle \tilde{u}(\bar{v}t - \gamma, h) \rangle_{\gamma, h} = 0$. Averaging \tilde{u} over γ is equivalent to averaging \tilde{u} for a fixed γ over a time period, T , with the result,

$$\begin{aligned} \langle \tilde{u} \rangle_\gamma &= \int_{t_J + nT}^{t_J + (n+1)T} \frac{dt}{T} \tilde{u}(\bar{v}t - \gamma, h) \\ &= \frac{F + \eta\bar{v}}{K} - \frac{h^2}{2K(K+h)} - \frac{(K+2h)\bar{v}}{\lambda(K+h)} - \frac{h^2}{K(K+h)} \frac{1}{e^{\lambda/\bar{v}} - 1}. \end{aligned} \quad (27)$$

Finally, averaging over h and using the consistency condition, we obtain

$$F - F_T = \bar{v}[1 - M(\eta, K)] + \left\langle \frac{h^2}{K(K+h)} \frac{1}{e^{(K+h)/(1+\eta)\bar{v}} - 1} \right\rangle_h, \quad (28)$$

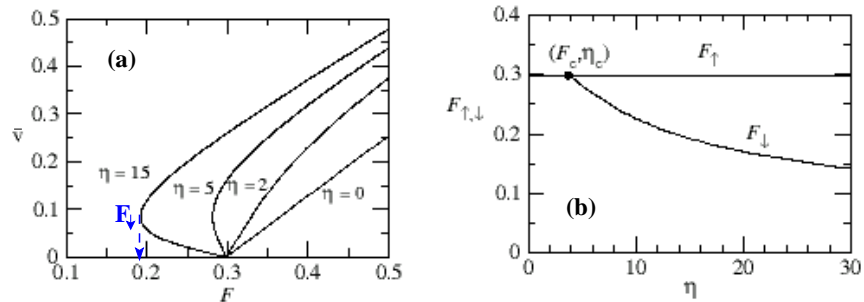


FIG. 5: (a) Velocity versus driving force for the VE model with $K = 1$ and a broad distribution of pinning strength, $\rho(h) = e^{-h}$. The velocity is continuous and single-valued for $\eta < \eta_c$ and becomes multivalued for $\eta > \eta_c$. The dashed line on the curve for $\eta = 15$ indicates the value F_{\downarrow} where the system repins when the drive is ramped down from the sliding state. Frame (b) shows the depinning and repinning forces F_{\uparrow} and F_{\downarrow} as functions of η . The tricritical point at (F_c, η_c) separates continuous from hysteretic depinning. Pinned and sliding states coexist in the region $F_{\downarrow} < F < F_{\uparrow}$.

with F_T the threshold force given in Eq. (25) and M given by

$$M(\eta, K) = (1 + \eta) \left\langle \frac{h^2}{(K + h)^2} \right\rangle_h. \quad (29)$$

As in the purely elastic case ($\eta = 0$) only static solutions exist for $F < F_T$. For $F > F_T$ there is a *unique* sliding solution, provided $M(\eta, K) < 1$, with mean velocity near threshold given by

$$\bar{v} \sim \frac{F - F_T}{1 - M(\eta, K)} \sim (1 + \eta_c) \frac{F - F_T}{\eta_c - \eta}, \quad (30)$$

giving $\beta = 1$, as in the purely elastic case. The critical line $\eta_c(K)$ separating unique from multi-valued sliding solutions is determined by $M(\eta, K) = 1$,

$$\eta_c(K) = \left\langle \frac{h^2}{(K + h)^2} \right\rangle_h^{-1} - 1. \quad (31)$$

The velocity-force curves and a phase diagram are shown in Fig. 5 for $\rho(h) = e^{-h}$. There is a *tricritical point* at $(\eta_c, F_c = F_T)$. In contrast to the purely viscous model with $K = 0$, for finite long-time elasticity ($K > 0$) the behavior is *independent of the shape of the pinning force distribution*, $\rho(h)$. For $\eta < \eta_c$, a continuous depinning transition at F_T separates a pinned state from a sliding state with *unique* velocity. In finite dimensions, this transition is likely to remain in the same universality class as the depinning of an elastic medium ($\eta = 0$). In our mean-field example, the linear response diverges at η_c , $v(\eta = \eta_c) \sim 1/\ln(F - F_T)$. For $\eta > \eta_c$ there is hysteresis with coexistence of stuck and sliding states.

Numerical simulations of the VE model in two dimensions ($d_{\parallel} = d_{\perp} = 1$) indicate a strong crossover (possibly a tricritical point) at a critical value of η_c from continuous to hysteretic depinning [27]. Although it is always difficult to establish conclusively on the basis of numerics that hysteresis survives in the limit of infinite systems, the size of the hysteresis loop evaluated numerically does appear to saturate to a finite value at large system sizes, indicating that the MF approximation may indeed capture the correct finite-dimensional physics.

V. RELATIONSHIP TO OTHER MODELS AND TO EXPERIMENTS

Other models of driven systems with inertial-type couplings have been proposed in the literature. It is useful to discuss in some detail their relationship to the viscoelastic model considered here.

In the context of charge density waves, Littlewood [15] and Levy and collaborators [16, 17] modified the Fukuyama-Lee-Rice model [4] that describes the phase of the CDW electrons as an overdamped elastic manifold driven through quenched disorder by incorporating the coupling of the CDW electrons to normal carriers. This was realized via a global coupling in the equation of motion for the phase to the mean velocity of the CDW, not unlike what obtained by a mean-field approximation of our viscous coupling. The model was argued to account for the switching and non-switching behavior observed in experiments.

Schwarz and Fisher [19, 25] recently considered a model of crack propagation in heterogeneous solids that incorporates stress overshoot, that is the fact that a moving segment of the crack can sometimes overshoot one or more potential static configurations before settling in a new one, inducing motion of neighboring segments. These effects may arise from elastic waves that can carry stress from one region to another of the driven medium. Stress overshoots, just like topological defects in a driven disordered lattice, have an effect similar to that of local inertia and were modeled by Fisher and Schwarz by adding couplings to gradients in the local crack velocity in the equation of motion for a driven elastic crack. These authors considered an automaton model where time is discrete. It is straightforward to define an automaton version of our VE model, where both the displacement u_i and time are discrete, as shown in Ref. [26]. It is then apparent that the automaton version of the viscoelastic model given in Ref. [26] is identical in its dynamics to the model of crack propagation with stress overshoot studied by Schwarz and Fisher, provided the strength M of the stress overshoot is identified with the combination $\eta/(1 + \eta)$. The two models differ in the type of pinning considered as the random force used in by Schwarz and Fisher is not periodic. We find, however, that the two models have identical mean-field behavior, with a mean-

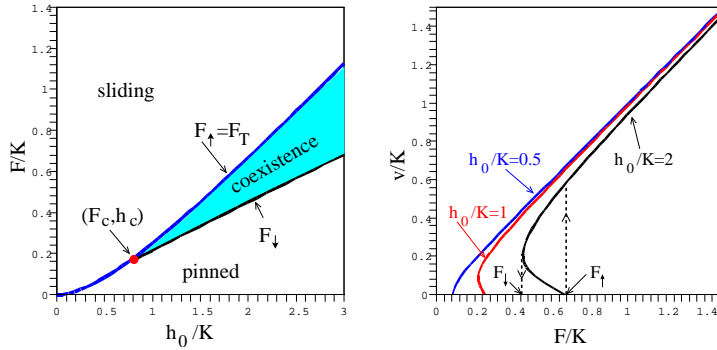


FIG. 6: Mean-field solution of the VE model with a piecewise parabolic pinning potential, $\rho(h) = \delta(h - h_0)$ and $\eta = 5$. Left frame: phase diagram. Right frame: velocity versus drive for $h_0/K = 0.5$ (blue), $h_0/K = 1$ (red) and $h_0/K = 2$ (black). Also shown for $h_0/K = 2$ are the discontinuous hysteretic jumps of the velocity obtained when F is ramped up and down adiabatically.

field tricritical point separating continuous from hysteretic dynamical transitions. The connection between the viscoelastic and the stress-overshoot model is important because it stresses that distinct physical mechanisms (inertia, nonlocal stress propagation, unbound topological defects) at play in different physical systems can be described generically by a coarse-grained model that includes a coupling to local velocities of the driven manifold. Finally, in a very recent paper, Maimon and Schwarz suggested that out of equilibrium a new type of generic hysteresis is possible even when the phase transition remains continuous [51]. Driven models with both elastic and dissipative velocity couplings may therefore belong to a novel universality class that exhibits features of both first and second order equilibrium phase transitions. They clearly deserve further study.

We now turn briefly to simulations and experiments. For comparison with experiments it is useful to point out that the tricritical point of the viscoelastic model can also be obtained by tuning the applied force and the disorder strength, rather than the applied force and the viscosity. Since the phase diagram does not depend on the form of the disorder distribution, $\rho(h)$, we choose for convenience a sharp distribution, $\rho(h) = \delta(h - h_0)$. The phase diagram in the (F, h_0) plane is shown in Fig. 6. For weak disorder the depinning is continuous, while for strong disorder it becomes hysteretic, with a region of coexistence of pinned and moving degrees of freedom. The *tricritical point* is at $(h_c, F_c = F_T)$, with $h_c = K/(\sqrt{1 + \eta} - 1)$.

Simulations of two-dimensional driven vortex lattices clearly show a crossover as a function of disorder strength from an elastic regime to a regime where the dynamics near depinning is spatially inhomogeneous and plastic, with coexistence of pinned and moving degrees of freedom

[39, 40, 52, 53]. In fact a bimodal distribution of local velocity was identified in Ref. [40] as the signature of plastic depinning. This local plasticity does not, however, lead to hysteresis in the macroscopic dc response in two dimension: the mean velocity remains continuous and single-valued, although it acquires a characteristic concave-up ward form near depinning that cannot be described by the exponent $\beta < 1$ predicted by elastic models in all dimensions. Hysteresis is, however, observed in simulations of three-dimensional layered vortex arrays where the couplings across layers are weaker than the in-layer ones [50]. In this case the phase diagram is qualitatively similar to that obtained for the viscoelastic model.

Recent experiments in $NbSe_2$ have argued that memory effects originally attributed in this system to "plasticity" of the driven vortex lattice [54] are actually due edge contamination effects [55, 56, 57]. In the experiments a metastable disordered vortex phase is injected in a stable ordered bulk vortex lattice. Memory effects may then arise in the macroscopic dynamics during the annealing of the injected disordered phase. Edge contamination does not, however, explain the plasticity seen in simulations, where periodic boundary conditions are used [40]. A possible scenario may be that while in the experiments the vortex lattice in the bulk is always in the ordered phase, in the simulations the vortex lattice in the bulk of the sample may be strongly disordered even in the absence of drive. Such a disordered vortex lattice would then naturally respond plastically to an external drive. Finally, it is worth mentioning one experimental situation where hysteresis of the type obtained in our model is indeed observed in the macroscopic response. This occurs in the context of charge density waves, driven by both a dc and an ac field. In this case the dc response exhibits mode-locking steps. The "depinning" from such mode-locked steps was found to be hysteretic [58].

Several colleagues and students have contributed to various aspects of this work: Alan Middleton, Bety Rodriguez-Milla, Karl Saunders, and Jen Schwarz. I am also grateful to Jan Meinke for help with some of the figures. The work was supported by the National Science Foundation via grants DMR-0305407 and DMR-0219292.

-
- [1] A. J. Liu and S. R. Nagel, *Nature* **391**: 21 (1998); A. J. Liu, this proceedings.
 - [2] D. S. Fisher, *Phys. Rep.* **301**: 113 (1998); and references therein.
 - [3] G. Blatter *et al.*, *Rev. Mod. Phys.* **66**: 1125 (1994).
 - [4] G. Grüner, *Rev. Mod. Phys.* **60**: 1129 (1988).

- [5] T. Giamarchi and S. Bhattacharya, in *High Magnetic Fields: Applications to condensed matter physics and spectroscopy*, C. Berthier et al., eds., p. 314 (Springer-Verlag, 2002).
- [6] E. Y. Andrei, Phys. Rev. Lett. **60**: 2765 (1988).
- [7] R. Seshadri and R. M. Westervelt, Phys. Rev. B **46**: 5142 & 5150 (1992).
- [8] D. S. Fisher, Phys. Rev. B **31**, 1396 (1985).
- [9] T. Giamarchi and P. Le Doussal, Phys. Rev. Lett. **72**: 1530 (1994); Phys. Rev. B **52**: 1242 (1995).
- [10] O. Narayan and D. S. Fisher, Phys. Rev. B **46**: 11520 (1992).
- [11] F. Nori, Science **271**: 1373 (1996).
- [12] A. Tonomura, Micron **30**: 479 (1999).
- [13] A. M. Troyanovski, J. Aarts and P. H. Kes, Nature **399**: 665 (1999).
- [14] A. Maeda, et al., Phys. Rev. B **65**: 054506 (2002).
- [15] P. B. Littlewood, Solid State Commun. **65**: 1347 (1988).
- [16] J. Levy, M. S. Sherwin, F. F. Abraham, and K. Wiesenfeld, Phys. Rev. Lett. **68**: 2968 (1992).
- [17] A. Montakhab, J. M. Carlson, and J. Levy, Phys. Rev. B **50**: 11227 (1994).
- [18] M. C. Marchetti, A. A. Middleton, and T. Prellberg, Phys. Rev. Lett. **85**: 1104 (2000).
- [19] J. M. Schwarz and D. S. Fisher, Phys. Rev. Lett. **87**: 096107 (2001).
- [20] M. C. Marchetti, A. A. Middleton, K. Saunders, and J. M. Schwarz, Phys. Rev. Lett. **91**: 107002 (2003).
- [21] S. H. Strogatz, C. M. Marcus, R. M. Westervelt, and R. E. Mirollo, Phys. Rev. Lett. **61**: 2380 (1988); Physica D **36**: 23 (1989).
- [22] V. M. Vinokur and T. Nattermann, Phys. Rev. Lett. **79**: 3471 (1997).
- [23] K. Saunders, J. M. Schwarz, M. C. Marchetti, and A. A. Middleton, Phys. Rev. B **69**: 37422 (2004).
- [24] M. C. Marchetti and K. A. Dahmen, Phys. Rev. B **66**: 214201 (2002).
- [25] J. M. Schwarz and D. S. Fisher, Phys. Rev. E **67**: 21603 (2003).
- [26] M. C. Marchetti, Pramana, to be published.
- [27] B. E. Rodriguez-Milla, M. C. Marchetti and A.A. Middleton, unpublished.
- [28] S. Zapperi, J. S. Andrade, Jr. and J. M. Filho, Phys. Rev. B **61**, 14791 (2000).
- [29] L. Balents. M. C. Marchetti and L. Radzihovsky, Phys. Rev. B **57**: 7705 (1998).
- [30] S. Scheidl, and V. M. Vinokur, Phys. Rev. E **57**: 2574 (1998).
- [31] T. Giamarchi and P. Le Doussal, Phys. Rev. B **57**: 11356 (1998).
- [32] Equation (11) should include a convective derivative that arises from the transformation to the laboratory frame [29]. This is negligible near a continuous depinning transition where the mean velocity is very small and it drops out in the mean field limit considered here. It will therefore be neglected, although it does play a crucial role on the dynamics well into the sliding state [29].
- [33] C. R. Myers and J. P. Sethna, Phys. Rev. B **47**: 11171 (1993).
- [34] A. A. Middleton, O. Biham, P. B. Littlewood, and P. Sibani: Phys. Rev. Lett. **68**, 1586 (1992).
- [35] A. A. Middleton, Phys. Rev. Lett. **68**: 670 (1992).

- [36] P. Le Doussal, K. J. Wiese, and P. Chauve, Phys. Rev. E **69**: 26112 (2004).
- [37] S. N. Coppersmith, Phys. Rev. Lett. **65**: 1044 (1990); Phys. Rev. B **44**: 2887 (1991).
- [38] S. N. Coppersmith and A. J. Millis, Phys. Rev. B **44**: 7799 (1991).
- [39] A.-C. Shi and A. J. Berlinsky, Phys. Rev. Lett. **67**: 1926 (1991).
- [40] M. C. Faleski, M. C. Marchetti and A. A. Middleton, Phys. Rev. B **54**: 12427 (1996).
- [41] L. Balents, M. C. Marchetti, and L. Radzihovsky, Phys. Rev. Lett. **78**: 751 (1997).
- [42] A. Zippelius, B. I. Halperin, and D. R. Nelson, Phys. Rev. B **22**: 2514 (1980).
- [43] See, for instance, D. R. Nelson in *Phase Transitions and Critical Phenomena*, C. Domb and J. Lebowitz eds. (Academic, London, 1983), Vol. 7, pp. 76-79.
- [44] M. C. Marchetti and K. Saunders, Phys. Rev. B **66**: 224113 (2002).
- [45] J. P. Boon and S. Yip, *Molecular Hydrodynamics* (McGraw-Hill, New York, 1980).
- [46] The strain-stress relation is nonlocal in both space and time. Only the nonlocality in time is retained here.
- [47] A. E. Koshelev and V. M. Vinokur, Phys. Rev. Lett. **73**, 3580 (1994).
- [48] K. Dahmen and J.P. Sethna, Phys. Rev. Lett. **71**: 3222 (1993); Phys. Rev. B **53**: 14872 (1996).
- [49] R. da Silveira and M. Kardar, Phys. Rev. E **59**: 1355 (1999).
- [50] C. J. Olson, C. Reichhardt and V. M. Vinokur, Phys. Rev. B **64**: 140502 (2001).
- [51] R. Maimon and J. M. Schwarz, Phys. Rev. Lett. **92**: 255502 (2004).
- [52] C. J. Olson, C. Reichhardt, and F. Nori, Phys. Rev. Lett. **81**: 3757 (1998).
- [53] N. Gronbech-Jensen, A. R. Bishop, and D. Dominguez, Phys. Rev. Lett. **76**: 2985 (1996).
- [54] S. Bhattacharya and M. J. Higgins, Phys. Rev. Lett. **70**: 2617 (1993); M. J. Higgins and S. Bhattacharya, Physica C **257**: 232 (1996).
- [55] Y. Paltiel, E. Zeldov, Y. N. Myasoedov, K. Shtrikman, S. Bhattacharya, M. J. Higgins, Z. L. Xiao, E. Andrei, P. L. Gammel, and D. J. Bishop, Nature **403**: 398 (2000).
- [56] Y. Paltiel, Y. Myasoedov, E. Zeldov, G. Jung, M.L. Rappaport, D. E. Feldman, M.J. Higgins, and S. Bhattacharya, Phys. Rev. B **66**: 60503 (2002).
- [57] M. Marchevsky, M. J. Higgins, and S. Bhattacharya, Phys. Rev. Lett. **88**: 87002 (2002).
- [58] M. J. Higgins, A. A. Middleton, and S. Bhattacharya Phys. Rev. Lett. **70**: 3784-3787 (1993)